*Journal of Thermal Analysis, Vol. 36 (1990) 869-880*

# THERMAL DECOMPOSITION OF BISHYDRAZINOCARBOXYLATE IRON(II) DI-HYDRAZINATE*

*K. B. Ghose, V. G. Gunjikar* and *S. K. Date*

PHYSICAL CHEMISTRY DIVISION, NATIONAL CHEMICAL LABORATORY, PUNE 411 008, INDIA

(Received January 9, 1989; in revised form April 26, 1989)

Low temperature ($T < 200°C$) thermal decomposition in air of bishydrazinocarboxylate iron(II) dihydrazinate [$Fe(II)(N_2H_3COO)_2(N_2H_4)_2$] is known to produce $\gamma$-$Fe_2O_3$ in ultrafine form [1-4]. This decomposition process is known to be exothermal and autocatalytic but details regarding the stepwise mechanism of decomposition is yet unknown although a few attempts have been made with limited success [1, 5]. In our present work, we have combined the results from (i) thermal analysis of complex precursor and (ii) characterization of products isolated at intermediate and final stages of decomposition in order to explain the stepwise mechanism of decomposition of $Fe(N_2H_3COO)_2(N_2H_4)_2$ in air.

## Experimental

Thermal stability of $Fe(N_2H_3COO)_2(N_2H_4)_2$ was studied in air as well as in nitrogen atmospheres by simultaneous recording of DTA/TG/DTG curves in NETZSCH STA 409 thermal analyzer. The first thermoanalytical curves (Fig. 1a) were recorded in dynamic air using around 25 mg sample heated at a rate of 10 deg/min. Since we failed to understand clearly the nature of these curves (A) due to overlapping of DTA peaks, other curves (B) (Fig. 1b) were recorded with $\approx$ 50 mg of sample heated at a rate of 5 deg/min. In nitrogen atmosphere, DTA, TG and DTG curves were recorded with $\approx$ 25 mg of sample heated at a rate of 5 deg/min, only to confirm the autocatalytic decomposition of the complex and will be referred to during the discussion, whenever necessary.

* NCL Communication No. 4613.

*John Wiley & Sons, Limited, Chichester*
*Akadémiai Kiadó, Budapest*

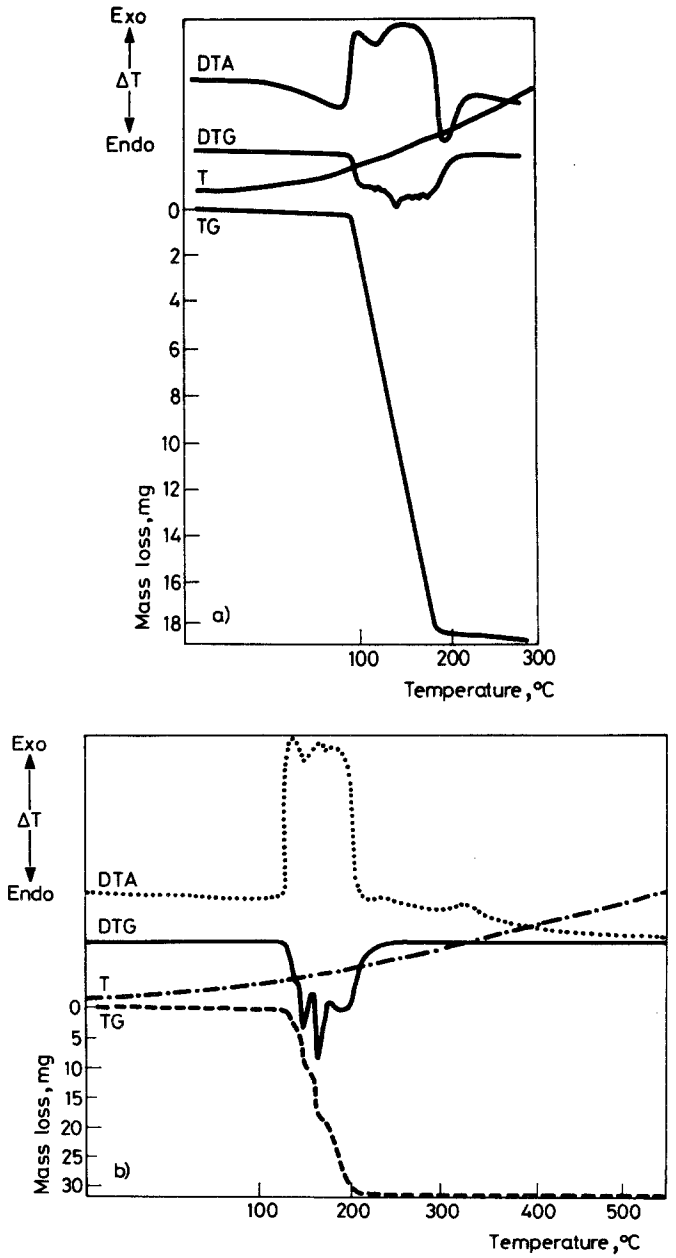


**Fig. 1** Thermoanalytical curves for the decomposition of $Fe(N_2H_3COO)_2(N_2H_4)_2$. a) in air - initial weight 24.15 mg; b) in air - initial weight 46.25 mg

The thermoanalytical curves B indicate precise temperature ranges at which major steps of decomposition occur in air. Accordingly, the intermediate and final decomposition products were isolated by stopping the reactions at those temperatures. These samples were characterised by infrared spectroscopy and X-ray diffraction analysis. Infrared (IR) spectra were recorded at room temperature on a Pye-Unicam SP-300 infrared spectrophotometer using nujol mulls and CsBr pellets. The characteristic group frequencies were identified by comparing the observed IR frequencies with those from standard IR data bank. X-ray diffractograms of powdered samples were recorded at room temperature by a Phillips PW 1730 X-ray diffractometer using $CuK_\alpha$ radiation with a nickel filter ($\lambda$ = 1.54 Å). The diffraction intensity was recorded as a function of angle of diffraction ($2\varphi$). The '*d*' values were calculated from Bragg relation

$$n\lambda = \frac{2d \text{ Sin } \theta}{hkl}$$

Different phases were identified by comparing the set of '*d*' values and corresponding intensities of diffraction with standards from ASTM data files.

## Results and discussion

According to earlier reports [1, 3], the complex $Fe(N_2H_3COO)_2(N_2H_4)_2$ deflagrates in air above 100° and undergoes exothermal, autocatalytic decomposition with evolution of large quantities of gases like $N_2$, $NH_3$, $N_2H_4$ to produce exclusively fine particles of $\gamma$-$Fe_2O_3$ as end product. The corresponding thermogram reportedly shows two exotherms and 70% total weight loss in a single step. Patil *et al.* [1] suggested that the sharp exotherm at $T \approx 130°$ corresponds to loss of coordinated $N_2H_4$ while the broad exotherm at $T \approx$ (160-180)° temperature range corresponds to decomposition of hydrazinocarboxylate ($N_2H_3COO^-$) groups. During the present work, we made a similar observation (Fig. 1a) only when the thermoanalytical curves (A) were recorded with lesser sample weight and faster heating rate. However, other curve (B) (Fig. 1b) recorded with more sample weight and slower heating rate exhibits four exothermal peaks (in DTA) and ≈ 70% total weight loss (in TG) in four steps. Results derived from analysis of thermoanalytical curves-B are presented in Table 1. Careful observation reveals that first three DTG curves are quite sharp and their line shapes are similar

indicating instantaneous decomposition of similar nature. The fourth DTG curve is broad showing decomposition of a relatively stronger bond of different nature. It is likely that the instantaneous processes correspond to expulsion of $N_2$, $NH_3$, $N_2H_4$ following rupture of N–Fe coordinate bonds while the slower process at higher temperature corresponds to rupture of Fe-O covalent bonds.

In order to identify the intermediate and final products of decomposition in air, the reaction was carried out three times separately and was stopped at 105°, 250° and 600° respectively. The products were isolated at respective temperatures and characterised by IR and XRD analyses. The results are discussed first for the product isolated at 250° followed by the remaining two products.

**Table 1** Results from DTA/TG/DTG of $Fe(N_2H_3COO)_2(N_2H_4)_2$ [Sample of 50 gms] in air

| Step No | Temp., °C | DTA | Features of DTG curve | TG weight loss, % Stepwise | | Accumulated |
|---|---|---|---|---|---|---|
| 1 | 139 | Sharp exotherm | Sharp | 10.80 | I | 10.80 |
| 2 | 152 | | Sharp | 16.96 | I+II | 25.94 |
| 3 | 164 | Broad exotherm | Sharp | 25.10 | I+II+III | 44.94 |
| 4 | 188 | | Broad | 41.30 | I+II+III+IV | 67.46 |
| 5 | 224 | Exotherm | - | - | | - |
| 6 | 321 | Exotherm | - | - | | - |

*a) Product isolated at 250°*

Infrared spectrum (Fig. 2b) of the sample shows two intense bands at ≈ 400 $cm^{-1}$ respectively whose lineshapes and positions are typical of those of a spinel ferrite [6, 7]. Iron oxides $Fe_3O_4$ and $\gamma$-$Fe_2O_3$ both are known to possess spinel structure. While pure magnetite shows two absorption bands at 575 $cm^{-1}$ and 380 $cm^{-1}$ respectively, additional bands at 390 $cm^{-1}$, 440 $cm^{-1}$, 554 $cm^{-1}$ and 635 $cm^{-1}$ appear for partially oxidized magnetite [8]. In the present case, broadness of the band at 380-450 $cm^{-1}$ and appearance of the extra band at 635 $cm^{-1}$ indicate formation of $\gamma$-$Fe_2O_3$ i. e. oxidized form of magnetite. Assignments of the observed frequencies to characteristic group frequencies [9] are provided in Table 2. The presence of surface hydroxyl group (≈ 3400 $cm^{-1}$) as indicated in the IR spectrum, agrees well with the fact that presence of water is essential for the stabilization of $\gamma$-$Fe_2O_3$ [10,

11]. It also shows that even if $Fe_3O_4$ were the sole product of decomposition initially, the presence of water on the fine particle surface has oxidized it (even if not completely) to $\gamma$-$Fe_2O_3$ and stabilized this metastable phase.

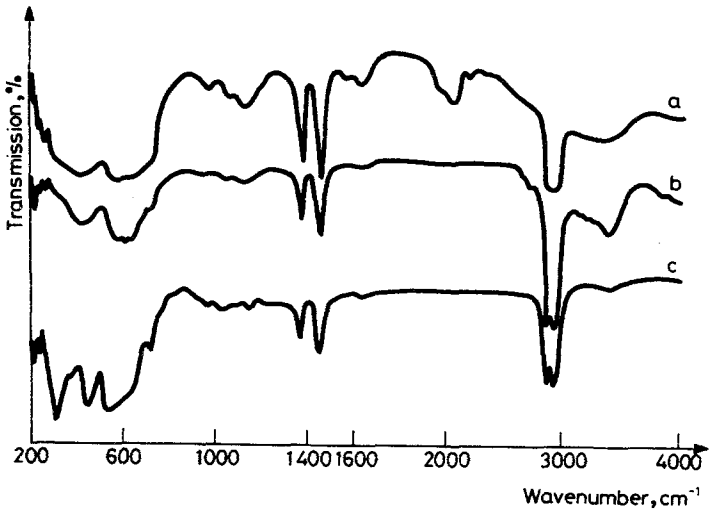


Fig. 2 Infrared absorption spectra for thermal decomposition (in air) products of $Fe(N_2H_3COO)_2(N_2H_4)_2$ isolated at various temperatures (a) 105°C, (b) 250°C and (c) 600°C

XRD pattern of the decomposition product matches with the patterns of both $\gamma$-$Fe_2O_3$ and $Fe_3O_4$ [12] because, difference between their lattice constants being small, both oxides show similar XRD patterns. In the present case, broadening of XRD lines makes it even more difficult to attribute the pattern to a particular oxide. Van Oosterhout [13] reported the presence of a few weak additional XRD lines for $\gamma$-$Fe_2O_3$ but such lines do not appear for ultrafine material [14, 15] which is the case presently. However, careful intensity analysis of the XRD lines and the absence of (222) line (typical for $Fe_3O_4$) [10] in the diffractogram of the decomposition product (Table 3) indicate a greater possibility of $\gamma$-$Fe_2O_3$ formation although simultaneous existence of a minor amount of $Fe_3O_4$ can not be ruled out.

These observations and the qualitative information obtained from the brown colour of the sample confirm the previously reported fact [1-5] that thermal decomposition of $Fe(N_2H_3COO)_2$ $(N_2H_4)_2$ in air produces ultrafine $\gamma$-$Fe_2O_3$.

*b) Product isolated at 600°*

The infrared spectrum of this compound (Fig. 2c) matches with that of haematite [16]. The frequency assignments are given in Table 2. The calculated '*d*' values and intensity analysis for it's X-ray diffractogram match with those single phase $\alpha$-$Fe_2O_3$ [12] as shown in Table 3.

**Table 2** Assignment of infrared absorption frequencies ($cm^{-1}$) for thermal decomposition products (isolated at 250° and 600°) of $Fe(N_2H_3COO)_2(N_2H_4)$ [Decomposition in air]

| Product isolated at 250°C | | Product isolated at 600°C | | |
|---|---|---|---|---|
| Frequency, $cm^{-1}$ | Assignment | Frequency, $cm^{-1}$ | | Assignment |
| 3400 | Surface OH stretching vibration | 725 | w, sp | |
| 720 | Lattice vibration | 530-580 | s, b | Lattice Fe-O vibrations |
| 640 | Fe-O bonding stretch | 440 | s, b | |
| 570 | Fe-O stretch at tetrahedral and octahedral site | 370<br>310 | s, b | |
| 380-450 | Fe-O at octahedral site | | | |

**Table 3** X-ray diffraction '*d*' values (Å) and relative intensities for thermal decomposition products in air (isolated at 250° and 600°) of $Fe(N_2H_3COO)_2(N_2H_4)_2$

| Product isolated at 250°C | | Product isolated at 600°C | |
|---|---|---|---|
| d, Å | $I/I_{max}$ | d, Å | $I/I_{max}$ |
| 2.95 | 35 | 3.67 | 28 |
| 2.52 | 100 | 2.69 | 100 |
| 2.09 | 22 | 2.51 | 75 |
| 1.70 | 7 | 2.20 | 23 |
| 1.60 | 25 | 1.84 | 36 |
| 1.48 | 39 | 1.69 | 44 |
| | | 1.60 | 10 |
| | | 1.48 | 26 |
| | | 1.45 | 26 |

*c) Product isolated at 105°*

The X-ray diffractogram of this sample matches with that of the reaction product isolated at 250° indicating the formation of an iron oxide spinel. The XRD lines are so broad that it is impossible to decide between $\gamma$-$Fe_2O_3$ and $Fe_3O_4$ as the possible product. In any case, it is obvious that even though the reaction is stopped at 105°, the complex has undergone autosus-

tained combustion to produce ultrafine $Fe_3O_4/\gamma$-$Fe_2O_3$. This can be explained in the following way: once a little iron oxide has formed, it may have catalysed the decomposition of hydrazinate complex [17] thereby dragging the reaction to near completion at a lower temperature. The extent of autosustained combustion is such that the yet undecomposed portion of the ferrous complex in the collected sample is less than sufficient to be detected by XRD analysis. Thus no other XRD line (except those for spinel oxide) appears in the diffractogram.

The infrared spectrum (Fig. 2a) of the sample shows a very broad band below 600 $cm^{-1}$ making specific assignment of absorption frequencies difficult. However, indications of the presence of two lattice vibration ($\approx$ 600 $cm^{-1}$, 400 $cm^{-1}$) show presence of $\gamma$-$Fe_2O_3/Fe_3O_4$ [8]. The broadness of the low frequency region speaks of the ultrafine nature of the material.

The IR bands appearing in the region above 600 $cm^{-1}$ are assigned (Table 4) on the basis of information obtained from IR spectroscopic analysis of original ferrous complex $Fe(N_2H_3COO)_2$ $(N_2H_4)_2$ (Table 4) and from relevant references [1, 18-10]. Careful analysis of the IR spectrum shows that the band due to unidentate $N_2H_4$ ($\sim$ 925 $cm^{-1}$) is completely absent while that due to $N_2H_3COO^-$ group ($\sim$ 980 $cm^{-1}$) is present at a reduced intensity. The other bands (at $\sim$ 3220 $cm^{-1}$, 1630 $cm^{-1}$, 1560 $cm^{-1}$, 1300 $cm^{-1}$, 1130 $cm^{-1}$, 1050 $cm^{-1}$) also have reduced intensities compared to corresponding bands for the original Fe-complex. The absence of $N_2H_4$ group and presence of trace amount of $N_2H_3COO^-$ group show that expulsion of $N_2H_4$ group takes place faster and at a lower temperature than the decomposition of $N_2H_3COO^-$ group.

The intense IR bands in the region around 200 $cm^{-1}$ may be assigned to characteristic vibrations of CO or $N_2$ groups [18]. Gas phase CO chemisorbed on iron surface has stretching frequencies in this region [20-24]. It is likely that gas phase CO, which is formed as a byproduct of decomposition, gets trapped on the surface of iron oxide. Obviously the ultrafine nature of iron oxide facilitates the process of adsorption.

Depending on above observations, we can propose that the intermediate decomposition product has an interlinked lattice of Fe-O with chemisorbed CO. A close analysis of (TG) weight losses at different stages of decomposition (Table 1) suggests that stoichiometric composition of this intermediate is possibly $FeO_2.2CO$. The product isolated at 105°C therefore comprises of a large portion of final product $\gamma$-$Fe_2O_3/Fe_3O_4$, intermediate product $FeO_2.2CO$ and a minor amount of undecomposed $N_2H_3COO^-$ group still bonded to iron.

**Table 4** Assignment of infrared absorption frequencies ($cm^{-1}$) of $Fe(N_2H_3COO)_2$ $(N_2H_4)_2$ and its thermal decomposition product (in air) isolated at 105°C

| $Fe(N_2H_3COO)_2$ $(N_2H_4)_2$ | | | Decomposition product | | |
|---|---|---|---|---|---|
| Frequency | | Assignment | Frequency | | Assignment |
| 3315 | m, vsp | $\gamma$ N–H ... O | 3150–3400 | w, vb | Surface hydroxyl, N–H stretching frequency |
| 3225 3150 | m, d | $\gamma$ (N–H) weakly H. bonded | | | |
| 2680 | w | N–H stretch | 2200 | w, sp | CO stretching frequency |
| 1650 | w | $\delta$ ($H_2O$) | 2040 | m, b | of gas phase carbonyl |
| | | | 1960 | m, sh | group |
| 1620 | s, b | $\delta$, ($NH_2$) bending | 1630 | w, b | $\delta$, ($NH_2$) bending |
| | | and $\gamma_{asymm.}$ | 1560 | w, b | $\gamma_{asymm.}$ $COO^-$ |
| 1580 | s b | $COO^-$ | | | |
| 1460 | s, b | $\gamma$ (C–N) stretching, | | | |
| 1390 | s, b | $\gamma$ $COO^-$ symm. | | | |
| 1340 | s, b | Stretch, $\delta$(NH) | 1300 | v, w | $\delta$(N–H) in plane bending, |
| | | in plane bending | | | $\gamma_{symm.}$ $COO^-$ |
| 1200 | s, h | $\rho_{NH_2}$ (twisting and wagging) | | | |
| 1110 | s, sp, d | $\gamma$ (C–N) stretch | 1130 | m, b | Overtone due to lattice |
| 1080 | | | 1050 | w, b | vibration, $\rho_{NH_2}$ (twisting and wagging) $\gamma$ (C–N) stretch |
| 980 | m, sp | $\gamma$ (N–N) for bidentate $N_2H_3COO^-$ ligand | 975 | w, b | $\gamma$ (N–N) due to bidentate $N_2H_3COO^-$, overtone due to lattice vibration |
| 920 | m, sp | $\gamma$ (N–N) for unidentate $N_2H_4$ | | | |
| 775 | s, sp | OCO bending, $\rho_r NH_2$ | | | |
| 720 | m, sp | $\rho_{COO^-}$ | | | |
| 640 | w, sh | $NH_2$ asymm. rocking, $\rho_{COO^-}$, | | | |
| 590 | vsp, s | $NH_2$ symm. rocking | 600 | s, vb | Lattice vibrations for Fe–O |
| | | $\delta COO^-$, $NH_2$ deformation | 400 | s, vb | Stretch |
| 420 | w, sh | $\gamma$ (Fe–N), $\delta$(C=O) | | | |
| 340 | m, sh | $\gamma$(Fe–N), $\delta$(C=O) | | | |
| 290 | s, sp | $\gamma$(Fe–O) | | | |

*Reaction mechanism*

As indicated earlier, the compositions of the isolated intermediates and final products of decomposition are now identified. On the basis of these results, it is possible to propose the following mechanism of decomposition (Table 5). The highlight of the proposed mechanism is the identification of the intermediate complex $FeO_2.2CO$ at step-3. Patil *et al.* [5] have earlier proposed the different steps during the thermal decomposition as

$$Fe(N_2H_3COO)_2\,(N_2H_4)_2 \rightarrow \underset{(I)}{FeC_2O_4\,(N_2H_4)_2}$$

$$\rightarrow \quad FeC_2O_4 \quad \rightarrow \quad Fe_2O_3$$

However, owing to the fast decomposition process, as we also have observed for the thermoanalytical curves (A) recorded with faster heating rate (Fig. 1a), they could not isolate the reaction intermediate (I) and identify it as such. The difference between the mechanism proposed by Patil *et al.* [5] and the one presented in this paper is due to the reaction intermediate which has actually been isolated and identified clearly as $FeO_2.2CO$.

It is apparent that the proposed course of reaction (Table 5) does not need external stimuli except for the partial pressure of oxygen at a latter stage to oxidize $Fe_3O_4$ to $\gamma$-$Fe_2O_3$. Therefore, when similar investigations are conducted in ordinary nitrogen atmosphere, the results are found to agree with those in air except for relatively slower rate and higher temperature of decomposition.

## Conclusion

It is found that the decomposition reaction in air of Fe(II) complex, $Fe(N_2H_3COO)_2(N_2H_4)_2$ proceeds following the mechanism:

$$[Fe(N_2H_3COO)_2(N_2H_4)_2 \rightarrow Fe(N_2H_3COO)_2 \rightarrow FeO_2.2CO]$$

$$FeO_2.CO \rightarrow Fe_3O_4 + \gamma Fe_2O_3 \xrightarrow[350-400^{\circ}C]{} \alpha\text{-}Fe_2O_3$$

**Table 5** Predicted course of decomposition of $Fe(N_2H_3COO)_2(N_2H_4)_2$ in air

| No of step | Predicted course of reaction | Comment | TG weight loss, % | | |
|---|---|---|---|---|---|
| | | | Stepwise | | Accumulated |
| | $Fe(N_2H_3COO)_2(N_2H_4)_2$ ↓ | Instantaneous process | | | |
| 1 | Loss of coordinated $N_2H_4$ ↓ | producing a sharp | 11.8 | I | 11.8 |
| | $Fe(N_2H_3COO)_2N_2H_4$ ↓ | DTG curve | | | |
| 2 | Loss of coordinated $N_2H_4$ ↓ | -do- | 13.4 | I+II | 23.7 |
| | $Fe(N_2H_3COO)_2$ ↓ | | | | |
| 3 | Loss of two $N_2H_3$ radicals as: $2N_2H_3 \rightarrow N_2 \uparrow + 2NH_3 \uparrow$ following clevage of coordinate and covalent bonds ↓ | -do- | 30.1 | I+II+III | 46.6 |
| 4 | $[FeO_2.2CO]$ Rupture of covalent bond, expulsion of CO, reorganization of lattice structure ↓ | Slow process showed by a broad DTG curve | | | |
| | (i) $\gamma$-$Fe_2O_3$ or | | (i) 44.44 or | I+II+III+IV or | 70.37 |
| | (ii) $Fe_3O_4$ ↓ | | (ii) 46.30 | I+II+III+IV | 71.36 |
| 5 | Oxidation of $Fe_3O_4$ part ↓ | Presence of adsorbed species masks the actual change in weight | | | |
| | $\gamma$-$Fe_2O_3$ ↓ | | | | + |
| 6 | Phase transition ↓ $\alpha$-$Fe_2O_3$ | Temp. and heat of transition are typical for this particular variety of $\gamma$-$Fe_2O_3$ since these parameters depend on the defect structure of the materials [26-28] which is itself variable for $\gamma$-$Fe_2O_3$ | | | |

Combining the IR and thermal data, it is possible to identify a reaction intermediate $FeO_2.2CO$ having interlinked lattice of iron oxide with gaseous CO trapped on its surface. In presence of air, $Fe_3O_4$ gets oxidized to $\gamma$-$Fe_2O_3$ at low temperature ($\approx 200^{\circ}$). It is also observed that presence of air expedites the combustion of the hydrazinate complex i. e. the decomposition reaction takes place much faster and at lower temperature than in inert (nitrogen) atmosphere. Ultrafine $\gamma$-$Fe_2O_3$ can thus be prepared exclusively from the precursor $Fe(N_2H_3COO)_2(N_2H_4)_2$ at sufficiently low temperature.

* * *

One of us (KBG) wishes to thank the Council of Scientific and Industrial Research for the award of the senior research fellowship. We are grateful to Dr. P. Ratnasamy for his continuing interest in our work.

## References

1 P. Ravidranathan and K. C. Patil, Proc. Indian Acad. Sci. (Chem. Sci.), 95 (1985) 345.
2 P. Ravindranathan and K. C. Patil, J. Materials Science Letters, 5 (1986) 221.
3 K. C. Patil, Proc. Indian Acad. Sci. (Chem. Sci.), 96 (1986) 459.
4 G. Bate, Magnetic Oxides, (D. J. Craik ed.) Wiley, London 1975; G. Bate, Ferromagnetic Materials, Vol. 2 (E. P. Wohlfarth ed.), North Holland Publishing Co., 1980.
5 K. C. Patil, D. Gajapathy and K. Kishore, Thermochim. Acta, 52 (1982) 113.
6 S. Hafner and Z. f. Krist., 115 (1961) 331.
7 R. D. Waldron, Phys. Rev., 99 (1955) 1727.
8 J. Gillot, J. Solid State Chem., 32 (1980) 303.
9 M. Ishii, M. Nakahira and T. Yamanaka, Solid State Commun., 11 (1972) 209.
10 J. David and A. J. E. Welch, Trans. Faraday Soc., 52 (1956) 1642; T. Elder, J. Appl. Phys. 36 (1965) 1012.
11 P. B. Braun, Naturel, 170 (1952) 1123; E. Hermann, Arhiv. Kemi., 22 (1950) 85; 23 (1951) 22.
12 ASTM data file.
13 G. W. Van Oosterhout and C. J. M. Rooijmans, Nature, 181 (1958) 44.
14 J. M. D. Coey and D. Khalafalla, Phys. Status Solidi, 11 (1972) 229.
15 K. Haneda and A. H. Morrish, Solid State Chem. Commun., 22 (1977) 779.
16 J. A. Gadsen, Infrared spectra of minerals and related inorganic compounds, 1975.
17 L. F. Audrieth and B. A. Ogg, The chemistry of hydrazine, John Wiley New York, 1952, p. 212.
18 A. Braibanti, F. Dallavalli, M. A. Pellinghelli and E. Leporati, Inorg. Chem., 7 (1968) 1430.
19 K. Nakamoto, Infrared spectra of inorganic and coordination complexes, N. Y. Wiley, 1963.
20 K. C. Patil, R. Soundararajan and V. R. Pai Verneker, Proc. Indian Acad. Sci. (Chem. Sci.), 88 (1979) 211.
21 D. W. Moon, S. L. Bernasek, D. J. Dwyer and J. L. Gland, J. Am. Chem. Soc., 107 (1985) 4363.
22 U. Seip, M. C. Tsai, K. Christmann, J. Kuppers and G. Ertl, Surf. Sci., 139 (1984) 29.
23 W. Erley, J. Vac. Sci. Technol., 18 (1981) 472.
24 J. Pritchard, Surf. Sci., 79 (1979) 231.
25 A. Ueno, T. Onish and K. Tamaru, Trans. Farad. Soc., 66 (1970) 756.
26 B. Mason, Geol. Foren Forhande, 65 (1943) 97.
27 A. Ferrier, Compt. Rend., 264C (1967) 819.
28 R. Schrader and M. Enke, Z. Anorg. Allgem. Chem., 323 (1965) 126.

**Zusammenfassung** — Mittels DTA/TG/DTG, XRD sowie IR wurde die thermische Zersetzung von Bis-hydrazinocarboxylat-eisen(II)-dihydrazinat untersucht. Die thermische Zersetzung verläuft in sechs Schritten und endet bei genügend niedriger temperatur mit der Bildung von $\gamma$-$Fe_2O_3$. Durch Auswertung der Untersuchungsdaten konnten die einzelnen Zwischenprodukte, darunter eine neuartige Verbindung $FeO_2.2CO$, identifiziert werden.